



## Kinetic study of Nafion degradation by Fenton reaction

Tomoko Sugawara, Norimichi Kawashima, Takuro N. Murakami\*

Faculty of Biomedical Engineering, Toin University of Yokohama, 1614, Kurogane-cho, Aoba-ku, Yokohama, Zip 225-8502, Japan

### ARTICLE INFO

#### Article history:

Received 18 August 2010  
Received in revised form 9 October 2010  
Accepted 18 October 2010  
Available online 3 November 2010

#### Keywords:

Nafion degradation  
Fenton reaction  
Kinetics  
Prediction  
Polymer electrolyte membrane

### ABSTRACT

To predict the durability of polymer electrolyte membranes in fuel cells, the degradation reactions of Nafion 117 films were studied as oxidation reactions with hydroxyl radicals as oxidation accelerators. The radical species were generated by the Fenton reaction between hydrogen peroxide ( $\text{H}_2\text{O}_2$ ) and iron ions ( $\text{Fe}^{2+}$ ). The Nafion degradation kinetics were estimated by fluorine ion ( $\text{F}^-$ ) generation. The  $\text{H}_2\text{O}_2$  and Nafion degradation reactions fit a pseudo-first-order rate constant. The values of the activation energy and frequency factor are  $85 \text{ kJ mol}^{-1}$  and  $3.97 \times 10^8 \text{ s}^{-1}$  for  $\text{H}_2\text{O}_2$  decomposition in the presence of a Nafion film and  $97 \text{ kJ mol}^{-1}$  and  $9.88 \times 10^8 \text{ s}^{-1}$  for  $\text{F}^-$  generation. The Nafion surface morphology became rough after reaction for 12 h; small cracks, approximately  $100 \mu\text{m}$  in length, were observed at temperatures below  $60^\circ\text{C}$ . These cracks connected to make larger gaps of approximately 1 mm at temperatures above  $70^\circ\text{C}$ . We also found a linear relationship between  $\text{H}_2\text{O}_2$  consumption and  $\text{F}^-$  generation. The rate constant is temperature dependent and expressed as  $\ln(d[\text{F}^-]/d[\text{decomposed } \text{H}_2\text{O}_2]) = -19.5 \times 10^3 \text{ K}^{-1} + 42.8$ .  $\text{F}^-$  generated and  $\text{H}_2\text{O}_2$  consumed along with the Nafion degradation conditions can be predicted using this relation.

© 2010 Elsevier B.V. All rights reserved.

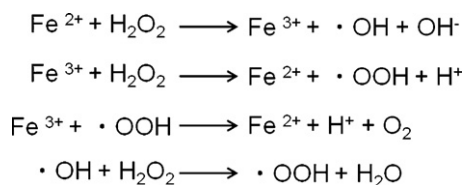
### 1. Introduction

Polymer electrolyte fuel cells (PEFCs) have recently been installed in houses as co-generation systems, and in future these systems will be used widely for supplying energy to cars and mobile electronic devices. PEFC technologies are still being developed to improve the cost effectiveness of PEFCs, their mass production techniques, and their lifetimes [1,2]. These issues have a large bearing on whether or not PEFCs are successfully commercialized. The cost of PEFCs should always be considered in conjunction with their lifetimes. The durability and aging of these cells have therefore been investigated [3–5]. Reports show that catalyst aggregation, degradation of the carbon electrodes, and decomposition of the polymer electrolyte could cause reductions in performance [6–10]. In particular, the polymer electrolyte membrane (PEM) has a strong influence on cell performances and lifetimes. The tearing of PEMs induces the crossover of both oxygen and hydrogen, decreasing cell efficiency. In addition, this oxygen leakage accelerates the degradation of the PEM at the anode caused by the production of hydrogen peroxide ( $\text{H}_2\text{O}_2$ ) [11–23]. Research on the degradation mechanisms of PEMs shows that the main damage to the polymers is the result of attack by the reactive oxygen species of free radicals such as hydroxyl radicals [3,24,25]. These reactive oxygen species are generated by reduction of  $\text{H}_2\text{O}_2$  with iron ions ( $\text{Fe}^{2+}$ ), as part of the

Fenton reaction (Scheme 1); in this reaction,  $\text{H}_2\text{O}_2$  is mostly produced at the anode by the catalytic combustion of the leaked oxygen and fuel hydrogen [15,18,19,26,27]. The  $\text{Fe}^{2+}$  released from the steel electrode or other metal ion contaminants also react with byproducts of  $\text{H}_2\text{O}_2$  at the anode [28].

In order to prevent membrane failure, research into the development and application of robust PEMs has been carried out [29–32]. In most PEFC research, however, Nafion, a commercially available polymer of perfluorinated sulfonic acid ionomers, is still employed as the PEM and for degradation studies. Reports on Nafion oxidation suggest that the reactive oxygen attacks the carboxyl groups at the chain ends and the sulfoxide groups on the side chains [3,12,15,22–25,32–34]. The oxidative degradation of the carboxyl group produces new carboxyl groups after decomposition of that group [26,27]. The polymer chain becomes shorter as a result of this cycle of unzipping reactions, the film finally becomes thinner, and pinholes appear [17,20]. The sulfoxide is a proton-transferring group and sulfoxide cleavage from the polymer decreases proton diffusion in the polymer. Although detailed research on the mechanisms has been conducted, quantitative details of reaction rates and kinetics have not been discussed and clarified until now. For example, there are few reports on the relationship between the degree of degradation and the concentration of  $\text{H}_2\text{O}_2$ , and most of the reports are simulation studies without any actual experimental results [26,27]. The occurrence of both radical reactions and polymer reactions make research on the kinetics of PEM decomposition reactions difficult. The reaction has several steps, and some factors such as diffusion of molecules and the reaction

\* Corresponding author. Tel.: +81 45 974 5135; fax: +81 45 972 5972.  
E-mail address: [murakami@edu.toin.ac.jp](mailto:murakami@edu.toin.ac.jp) (T.N. Murakami).



Scheme 1. Fenton reaction.

order are complicated. However, the degradation dependence on the  $\text{H}_2\text{O}_2$  concentration and on the reaction temperature will be useful information for predicting PEM damage in cells because it is difficult to see the condition of the PEM in the cell after assembly.

We have therefore tried to find the relationship between the decomposition level of Nafion 117, which is commonly used as a PEM, and  $\text{H}_2\text{O}_2$  decomposition, using an accelerated Fenton reaction at different temperatures. The actual equation for the reaction rate of Nafion ionomer would be complex because diffusion coefficients of the reactants are possibly different between in the bulk and on the surface of the polymer [26,27]. However, in this study, we employ the reaction rates correspond to the homogeneous rate constant to consider the reaction as simple. The decomposition of the Nafion is estimated from the released fluorine ion ( $\text{F}^-$ ) concentration. The reaction orders are approximated as pseudo-first order for simplicity. The reaction rate constant for  $\text{H}_2\text{O}_2$  decomposition by the Fenton reaction is plotted on an Arrhenius diagram to estimate both the activation energy and the reaction temperature dependence. The change in the surface morphologies of the Nafion film in several oxidation states at different reaction temperatures are also compared. Finally, the relationship between the Nafion and  $\text{H}_2\text{O}_2$  degradation rates is investigated using the fluorine ion concentration and the  $\text{H}_2\text{O}_2$  concentration.

## 2. Experimental

Nafion 117 membranes (DuPont, Wilmington, DE, USA), 175  $\mu\text{m}$  thick and of area 15 mm  $\times$  20 mm, were cleaned by thrice immersing the membranes for 1 min in ultrapure water and ethanol alternately. They were then dried in a vacuum desiccator for 1 h at room temperature. The other chemical reagents were used without further purification.

The Fenton reaction, i.e., the reduction of  $\text{H}_2\text{O}_2$  by  $\text{Fe}^{2+}$  ions, was used to generate hydroxyl radicals. An aqueous solution of iron(II) sulfate heptahydrate (Kanto Chemical Co., Inc., Tokyo, Japan) was added to 9.68 M  $\text{H}_2\text{O}_2$  (phosphate < 0.05 ppm, Wako Pure Chemical Industries, Ltd., Osaka, Japan) to produce a 0.36 mM  $\text{Fe}^{2+}$  aqueous solution. The membranes were oxidized by immersion in this solution.

The concentration of  $\text{H}_2\text{O}_2$  in the reaction solution was measured by complexation with titanium(IV) sulfoxide and measurement of the visible light absorption at 407 nm. The titanium(IV) sulfoxide solution was prepared from a mixture of 0.86 M titanium(IV) oxysulfate (Aldrich, St Louis, MO, USA), 0.30 M ammonium sulfate (Kanto Chemical Co., Inc.), and 2.04 M sulfuric acid (Wako Pure Chemical Industries, Ltd.). This solution was heated carefully until all the solids had dissolved and then cooled and diluted with distilled water. The sample solutions obtained as a result of Fenton reaction were added to the titanium(IV) sulfoxide solution and heated at 60  $^\circ\text{C}$  for 10 min to form a complex. The absorption of the solution at 407 nm was measured with a UV–vis spectrometer (V550, JASCO, Tokyo, Japan).

The fluoride ion concentration was measured with a fluoride ion meter (TiN-5101, Toko Chemical Laboratories Co., Ltd., Tokyo, Japan). The morphology of the film surface was observed by scan-

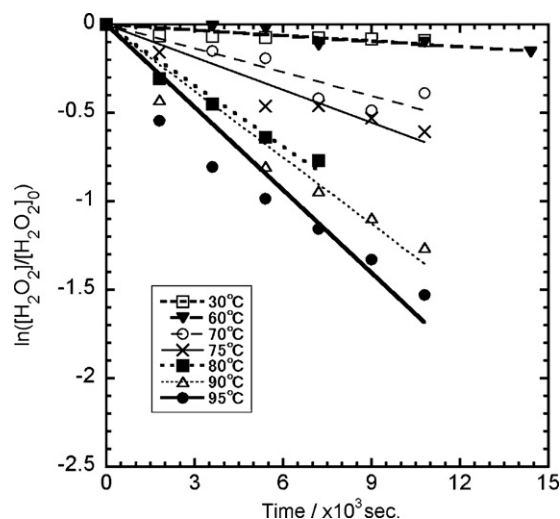


Fig. 1. Decomposition rate of  $\text{H}_2\text{O}_2$  as natural logarithmic function in the reaction with iron(II) sulfate. Initial concentrations of  $\text{H}_2\text{O}_2$  and iron(II) sulfate are 9.68 M and 0.36 mM, respectively; reaction temperatures are 30  $^\circ\text{C}$  ( $\square$ ), 60  $^\circ\text{C}$  ( $\blacktriangledown$ ), 70  $^\circ\text{C}$  ( $\circ$ ), 75  $^\circ\text{C}$  ( $\times$ ), 80  $^\circ\text{C}$  ( $\blacksquare$ ), 90  $^\circ\text{C}$  ( $\triangle$ ), and 95  $^\circ\text{C}$  ( $\bullet$ ). The plots approximate a pseudo-first-order rate constant.

ning electron microscopy (SEM; JSM-5500LV, JEOL, Tokyo, Japan) and atomic force microscopy (AFM; SPA400, Seiko Instruments, Inc., Chiba, Japan).

## 3. Results and discussion

The Fenton reaction is outlined in Scheme 1.  $\text{H}_2\text{O}_2$  is reduced by iron(II) ions ( $\text{Fe}^{2+}$ ), resulting in the formation of hydroxyl radicals ( $\text{OH}^\bullet$ ), hydroxide ions, and iron(III) ions ( $\text{Fe}^{3+}$ ) [3,26,27]. In this study, the Fenton reaction is used to generate hydroxyl radicals, which in turn are used to oxidize the Nafion film. The  $\text{H}_2\text{O}_2$  decomposition rates are measured at different reaction temperatures to determine the kinetics of the reaction. It has been confirmed that the concentration of  $\text{H}_2\text{O}_2$  does not change significantly during heating at 95  $^\circ\text{C}$  without Fenton reaction but it could be reduced 8% by initial heating in preparation of the reaction solution (see supplementary data). Fig. 1 shows the natural logarithm of the  $\text{H}_2\text{O}_2$  concentration in the Fenton reaction, normalized with respect to the initial concentration. The plots are fitted as pseudo-first-order rate constants to estimate the decomposition rate. The  $\text{H}_2\text{O}_2$  concentration at each reaction temperature has a good linear relationship with the reaction time. In order to determine the effect of Nafion on the  $\text{H}_2\text{O}_2$  consumption, the decomposition rates of  $\text{H}_2\text{O}_2$  in the presence of Nafion were also measured. The film was immersed in the reaction solution under the same conditions as in the reaction without Nafion. Fig. 2 shows the  $\text{H}_2\text{O}_2$  concentration in the reaction with Nafion at each reaction temperature. These results also give a good linear relationship with reaction time as a pseudo-first-order rate constant. The  $\text{H}_2\text{O}_2$  consumption rate constants in the simple Fenton reaction are compared with those for the same reaction in the presence of Nafion. The rate constants, correlation factors, and half-life times are shown in Table 1. The correlation factors are higher than 0.85, except for the reaction at 30  $^\circ\text{C}$  without Nafion. There are no significant differences between the correlation factors. However, the rate constants for the reactions with Nafion are higher than those for the reactions without Nafion at temperatures in the range of 60–95  $^\circ\text{C}$ . The results show that Nafion accelerates the  $\text{H}_2\text{O}_2$  decomposition. These differences can be explained by the reduction of  $\text{Fe}^{3+}$  to regenerate  $\text{Fe}^{2+}$ . The reduction of  $\text{Fe}^{3+}$  by organic radicals is quite possible. In this case, organic radicals such as fluorocarbon radicals ( $\text{CF}_2^\bullet$ ), released as a

**Table 1**

Difference of pseudo-first-order rate constants,  $k$ , in the presence of Nafion in  $\text{H}_2\text{O}_2$  decomposition reaction.  $R^2$  and  $t_{1/2}$  correspond to the correlation factor and half-life time, respectively.

| Temperature ( $^{\circ}\text{C}$ ) | Without Nafion                      |       |                                   | With Nafion                         |       |                                   |
|------------------------------------|-------------------------------------|-------|-----------------------------------|-------------------------------------|-------|-----------------------------------|
|                                    | $k (\times 10^{-3} \text{ s}^{-1})$ | $R^2$ | $t_{1/2} (\times 10^3 \text{ s})$ | $k (\times 10^{-3} \text{ s}^{-1})$ | $R^2$ | $t_{1/2} (\times 10^3 \text{ s})$ |
| 30                                 | $1.02 \times 10^{-2}$               | 0.25  | 68.0                              | $5.51 \times 10^{-3}$               | 0.94  | 126                               |
| 60                                 | $1.04 \times 10^{-2}$               | 0.90  | 66.6                              | $3.17 \times 10^{-2}$               | 0.85  | 21.9                              |
| 70                                 | $4.50 \times 10^{-2}$               | 0.99  | 15.4                              | $5.03 \times 10^{-2}$               | 0.87  | 13.8                              |
| 75                                 | $6.16 \times 10^{-2}$               | 0.98  | 11.3                              | $7.10 \times 10^{-2}$               | 0.99  | 9.76                              |
| 80                                 | $1.15 \times 10^{-1}$               | 0.96  | 6.03                              | $1.02 \times 10^{-1}$               | 0.94  | 6.80                              |
| 90                                 | $1.25 \times 10^{-1}$               | 0.94  | 5.55                              | $2.51 \times 10^{-1}$               | 0.99  | 2.76                              |
| 95                                 | $1.56 \times 10^{-1}$               | 0.89  | 4.44                              | $5.04 \times 10^{-1}$               | 0.95  | 1.38                              |

result of decomposition of Nafion, could promote reduction of  $\text{Fe}^{3+}$  to  $\text{Fe}^{2+}$ .

The reaction rate constants at temperatures in the range of 60–96  $^{\circ}\text{C}$  were drawn as Arrhenius plots in Fig. 3, and the plots fitted to the Arrhenius equation:

$$\ln k = \ln A - \left( \frac{E_a}{RT} \right)$$

In the equation,  $k$  is the rate constant of the reaction,  $A$  is the frequency factor, which depends on the probabilities of molecular collisions and the orientations of the collisions, and  $E_a$ ,  $R$ , and  $T$  are the activation energy, the gas constant, and the absolute temperature, respectively. The Arrhenius parameters give the activation energy for decomposition of  $\text{H}_2\text{O}_2$  in the Fenton reaction. The correlation factors in presence of Nafion and without Nafion, obtained by fitting to the Arrhenius equation, are determined as 0.93 and 0.89, respectively. The activation energy and the frequency factor are  $85 \text{ kJ mol}^{-1}$  and  $3.97 \times 10^8 \text{ s}^{-1}$  in the presence of Nafion, and  $72 \text{ kJ mol}^{-1}$  and  $2.96 \times 10^6 \text{ s}^{-1}$  without Nafion. The  $E_a$  of the reaction with Nafion is about  $10 \text{ kJ mol}^{-1}$  higher than that of the reaction without Nafion. This means that the presence of Nafion results in a stronger dependence on the reaction temperature for  $\text{H}_2\text{O}_2$  decomposition. In addition, Nafion could be a radical scavenger, controlling the attack of reactive oxygen on  $\text{H}_2\text{O}_2$ . This reaction could increase the activation energy. On the other hand, the frequency factor of the reaction with Nafion is about 100 times higher than that without Nafion. This indicates that Nafion increases the

probability of  $\text{H}_2\text{O}_2$  decomposition. This result supports the suggestion that Nafion produces sufficient radicals to reduce  $\text{Fe}^{3+}$  to  $\text{Fe}^{2+}$  and to attack  $\text{H}_2\text{O}_2$  directly.

The fluoride ion concentration in the reaction solution is a significant parameter because the release of fluoride ions results in damage to the main chain and the side chain of Nafion. The degradation of Nafion was estimated from the concentration of fluoride ions in solution. The film was immersed in the Fenton reaction solution at temperatures in the range of 30–95  $^{\circ}\text{C}$ . The fluoride ion concentration increased exponentially with reaction time. The fluoride ion concentration reaches saturation after approximately 230 min and 120 min at 90  $^{\circ}\text{C}$  and 95  $^{\circ}\text{C}$ , respectively. In contrast, the  $\text{H}_2\text{O}_2$  is consumed in 220 min at 90  $^{\circ}\text{C}$  and in 100 min at 95  $^{\circ}\text{C}$ . These results demonstrate that fluoride ion generation can be stopped by complete decomposition of  $\text{H}_2\text{O}_2$  and that Nafion cannot be damaged without  $\text{H}_2\text{O}_2$ , even after oxidation. The concentration of the reactants is an important parameter in the kinetic study. However, Nafion is present as a polymer film in this reaction and determining the initial concentration of the polymer is difficult. We therefore defined the initial concentration of the fluorine group in the Nafion film as the maximum concentration of the fluoride ion after oxidation in discussions of the reaction rate and in the Arrhenius plot. Fig. 4 shows the decomposition rate of fluorine groups in Nafion at each reaction temperature. The plots are fitted as pseudo-first-order rate constants to estimate the decomposition rate of the fluorine groups. The pseudo-first-order rate equation is

$$\ln \left( \frac{[\text{NaF}^*] - [\text{F}^-]}{[\text{NaF}^*]} \right)$$

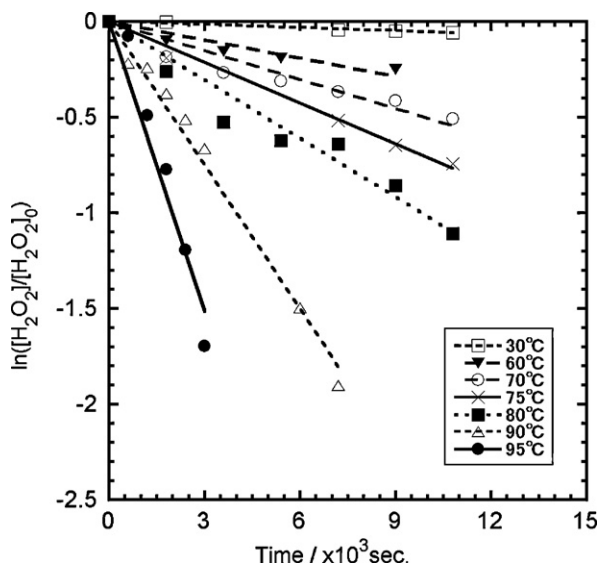


**Fig. 2.** Decomposition rate of  $\text{H}_2\text{O}_2$  as natural logarithmic function in the reaction with iron(II) sulfate in the presence of Nafion. Initial concentrations of  $\text{H}_2\text{O}_2$  and iron(II) sulfate are 9.68 M and 0.36 mM, respectively; reaction temperatures are 30  $^{\circ}\text{C}$  ( $\square$ ), 60  $^{\circ}\text{C}$  ( $\blacktriangledown$ ), 70  $^{\circ}\text{C}$  ( $\circ$ ), 75  $^{\circ}\text{C}$  ( $\times$ ), 80  $^{\circ}\text{C}$  ( $\blacksquare$ ), 90  $^{\circ}\text{C}$  ( $\triangle$ ), and 95  $^{\circ}\text{C}$  ( $\bullet$ ). The plots approximate a pseudo-first-order rate constant.

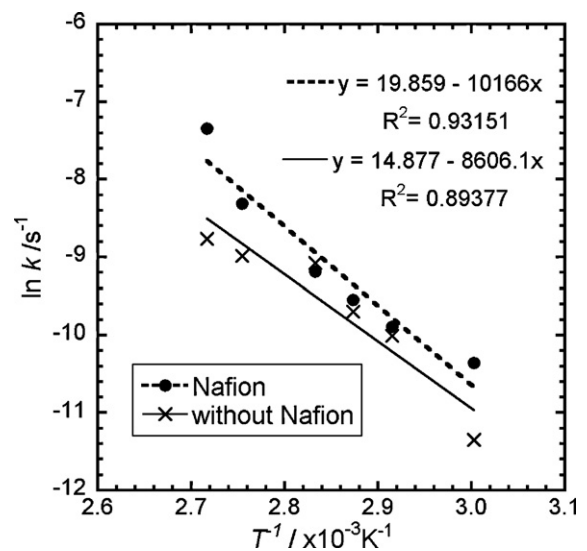


**Fig. 3.** Arrhenius plots of  $\text{H}_2\text{O}_2$  decomposition reaction with and without Nafion in the reaction solution.  $\bullet$ : Nafion in the reaction solution,  $\times$ : solution without Nafion.

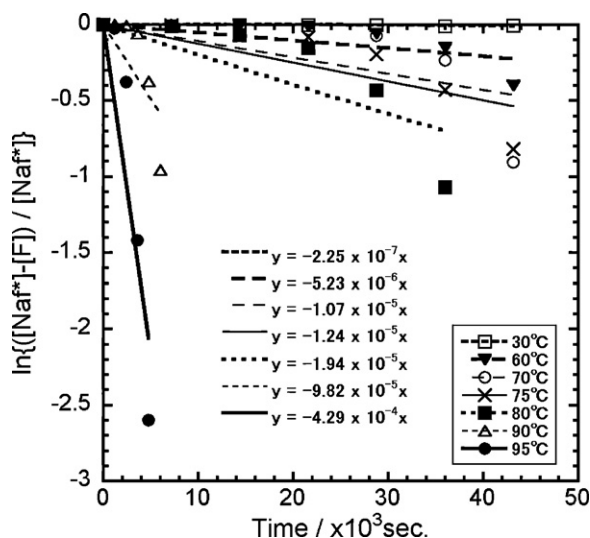


Fig. 4. Decomposition rate of fluoride ion as natural logarithmic function.  $[NaF^*]$  equals the maximum  $F^-$  ion concentration at 95 °C. The reaction temperatures are 30 °C (□), 60 °C (▼), 70 °C (○), 75 °C (×), 80 °C (■), 90 °C (△), and 95 °C (●).

The initial concentration of fluorine groups in Nafion is expressed as  $[NaF^*]$  and this is defined as the maximum concentration of fluoride ions at 95 °C after saturation. The concentration of fluorine groups during the reaction is defined as the difference between the initial concentration of fluorine groups and the fluoride ion concentration in the reaction, and is expressed as  $[NaF^*] - [F^-]$ .

The relationship between the decrease in fluorine groups and the reaction temperature is shown in Fig. 5. The reaction rate constants are plotted against inverse Kelvin temperature and the plots

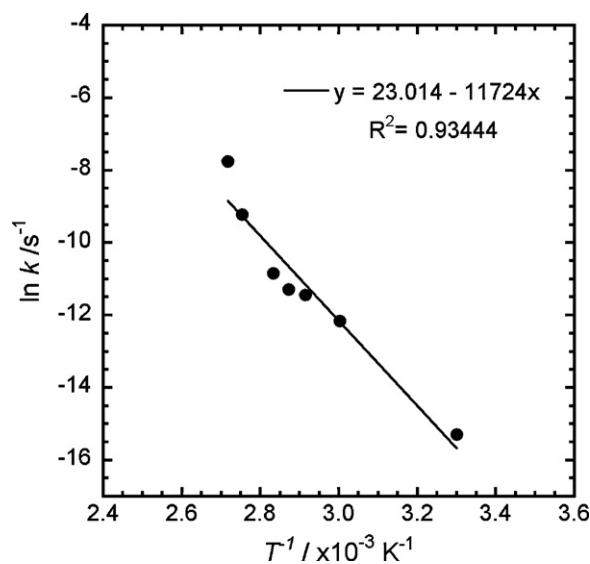


Fig. 5. Arrhenius plots of Nafion decomposition in the reaction between  $H_2O_2$  and iron(II) sulfate.  $k$  is calculated as a pseudo-half-order rate constant.

are fitted to the Arrhenius equation. The relation shows a good correlation and the correlation factor is 0.9. The activation energy of the decomposition reaction of fluorine groups in Nafion and the frequency factor from Fig. 5 are  $97 \text{ kJ mol}^{-1}$  and  $9.88 \times 10^9 \text{ s}^{-1}$ , respectively.

Hydrofluoric acid (HF), one of the decomposition products in the reaction, is a volatile compound and the concentration might be changed with heating. To confirm this effect, the concentration of HF in simple aqueous solution was measured under heat-

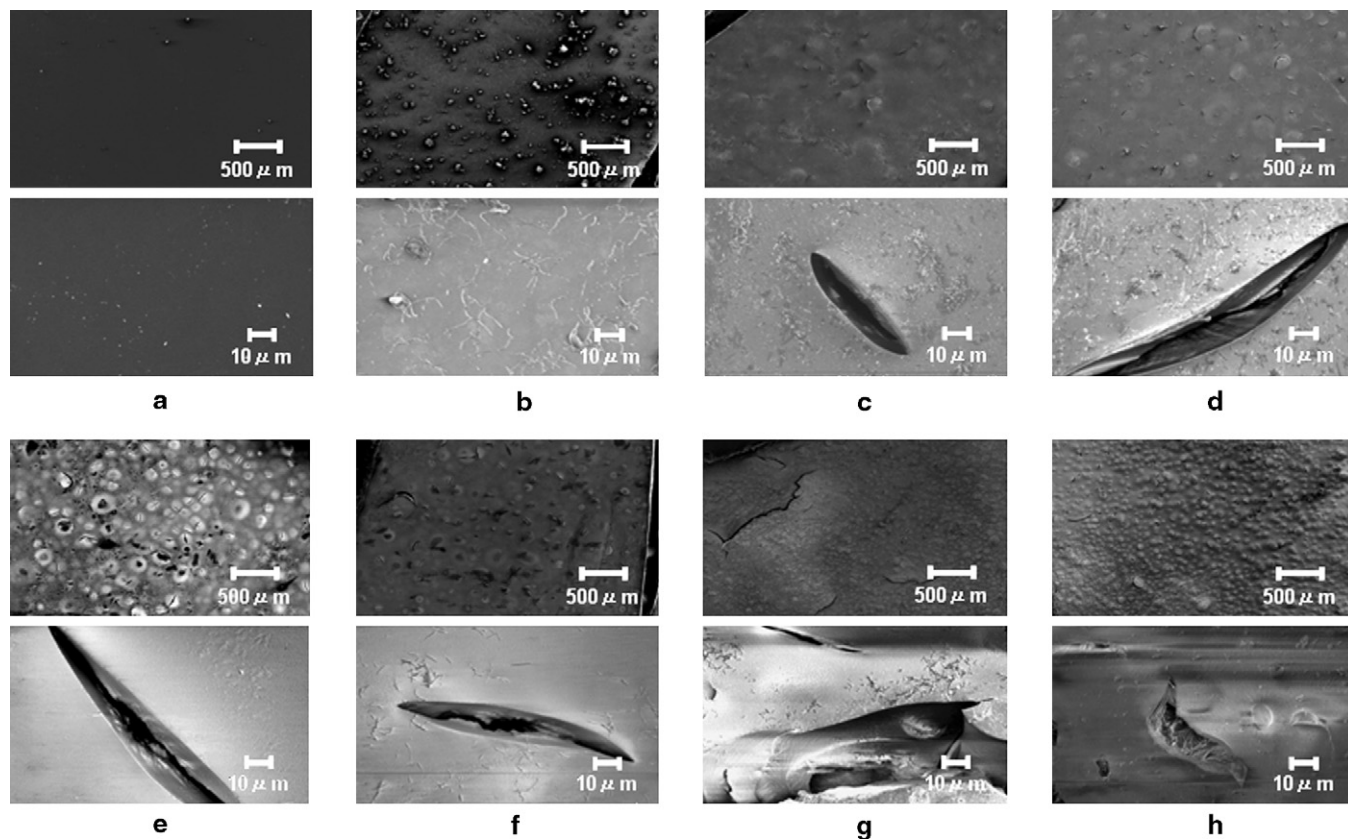


Fig. 6. SEM images of Nafion (a), and the film after reaction for 12 h at 30 °C (b), 60 °C (c), 70 °C (d), 75 °C (e), 80 °C (f), 90 °C (g), and 95 °C (h).



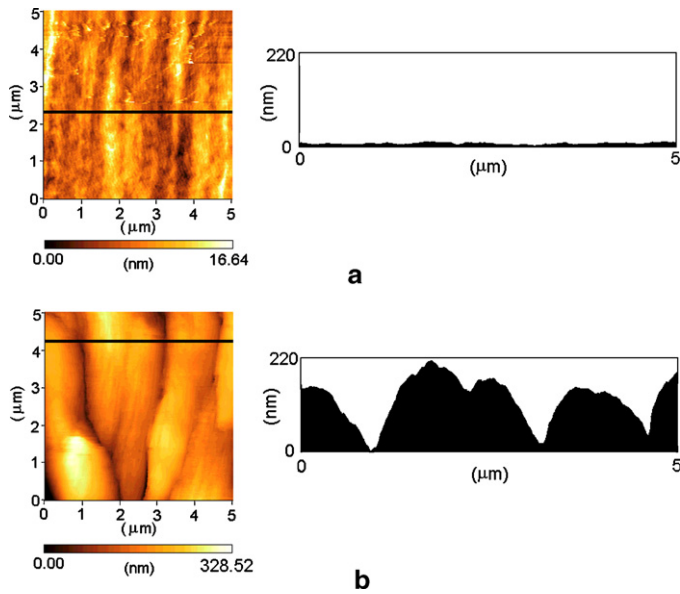


Fig. 7. AFM images of treated Nafion films with a height profile across the line shown in the image. (a) The film before treatment, (b) after treatment for 12 h at 90 °C.

ing at 95 °C. The initial concentration of HF,  $4.73 \times 10^{-3} \text{ mol L}^{-1}$ , slightly decreases with heating and becomes  $4.14 \times 10^{-3} \text{ mol L}^{-1}$  in  $34.2 \times 10^3 \text{ s}$ . The reduction rate is  $-0.27\%$  per 1000 s at 95 °C from the equation of linear approximation (see supplementary data). This is negligible to discuss the reaction rate constant in this research.

The PEMs in aged PEFCs experience morphological damage, for example tearing of the film [17–20]. Small cracks and pinholes in thin PEMs can cause gas-leakage problems. These changes in the morphology of the PEM are also related to oxidation reactions with reactive oxygen. The relationship between oxidation reactions and the surface profile of the Nafion film was examined by SEM; images of the film surfaces are shown in Fig. 6. Some cracks are observed in the Nafion after reaction and the number of cracks increases with reaction temperature; however, the size of the cracks is ca.  $100 \mu\text{m}$  and the size does not differ much with reaction temperature. The growth of cracks in the film can be considered to proceed by connection of a number of cracks of limited size to make a larger gap. The surface profiles of the desiccated film were also observed by AFM of a  $5 \mu\text{m} \times 5 \mu\text{m}$  area, and are shown in Fig. 7. After the treatment, the Nafion has an obviously rough surface and the gap depth is about 200 nm for the film which underwent reaction at 95 °C for 12 h. The oxidation reaction causes cleavage and scrapes material from the Nafion surface.

The hydroxyl radical and other oxidation radicals are highly reactive chemical species and quantitative analysis of hydroxyl radicals and other active oxygen species is difficult. These radicals react quickly with neighboring molecules, for example, the half-lives of hydroxyl radicals and superoxides in a 1 mM aqueous solution substrate are 7  $\mu\text{s}$  and 7 ms, respectively. On the other hand, the number of hydroxyl radicals generated is related to the amount of decomposed  $\text{H}_2\text{O}_2$ . We therefore tried to find the relation between  $\text{H}_2\text{O}_2$  consumption and Nafion degradation from the fluoride ion concentration. In Fig. 8, the fluoride ion concentration is plotted as the amount of decomposed  $\text{H}_2\text{O}_2$  at each reaction temperature, and the parameters of the approximation line obtained by the least-squares method are listed in Table 2. Some of the parameters have good correlation with  $\text{H}_2\text{O}_2$  decomposition and fluoride ion concentration. Interestingly, this relation is also temperature dependent. This means that the reaction temperature is an important factor in Nafion degradation; even if the same

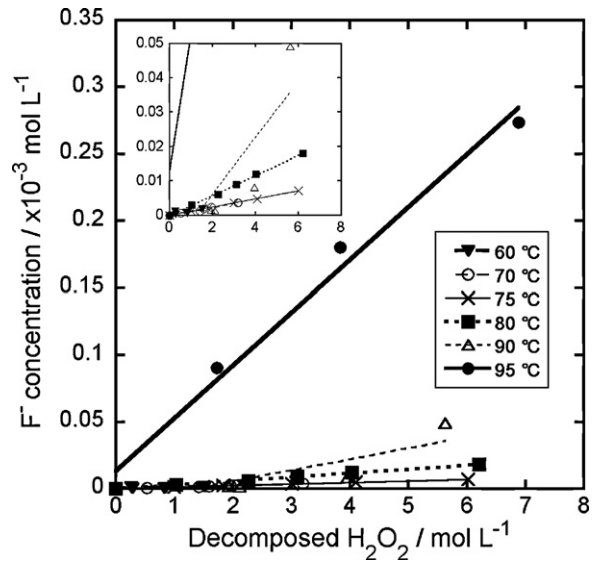


Fig. 8. Relation between the amount of decomposed  $\text{H}_2\text{O}_2$  and concentration of fluoride ions at different temperatures: 60 °C ( $\blacktriangledown$ ), 70 °C ( $\circ$ ), 75 °C ( $\times$ ), 80 °C ( $\blacksquare$ ), 90 °C ( $\triangle$ ), and 95 °C ( $\bullet$ ). The inset shows the small range of  $\text{F}^-$  concentrations.

Table 2

The parameter of the approximation line in Fig. 8 by the least-squares method.  $d[\text{F}^-]/d[\text{H}_2\text{O}_2]$  indicates the rate of  $\text{F}^-$  concentration increase with respect to  $\text{H}_2\text{O}_2$  concentration.

| Temperature (°C) | $d[\text{F}^-]/d[\text{H}_2\text{O}_2]$ | Intercept of $[\text{F}^-]$ | $R^2$ |
|------------------|---|-----------------------------|-------|
| 60               | $9.20 \times 10^{-7}$                   | $2.27 \times 10^{-7}$       | 0.78  |
| 70               | $1.14 \times 10^{-6}$                   | $-5.91 \times 10^{-8}$      | 0.99  |
| 75               | $1.18 \times 10^{-6}$                   | $5.32 \times 10^{-8}$       | 0.99  |
| 80               | $2.93 \times 10^{-6}$                   | $-1.23 \times 10^{-7}$      | 0.99  |
| 90               | $8.19 \times 10^{-6}$                   | $1.03 \times 10^{-5}$       | 0.83  |
| 95               | $3.94 \times 10^{-5}$                   | $1.33 \times 10^{-5}$       | 0.99  |

amounts of  $\text{H}_2\text{O}_2$  are consumed, the degradability increases with temperature.

The relations between  $\text{H}_2\text{O}_2$  decomposition and fluoride ion formation with reaction temperature could provide very useful information for predicting the condition of the Nafion film in a cell. We therefore plotted the rates of fluoride ion concentration with respect to  $\text{H}_2\text{O}_2$  consumption for cases where the correlation factors were higher than 0.9 (Table 2) against the inverse of

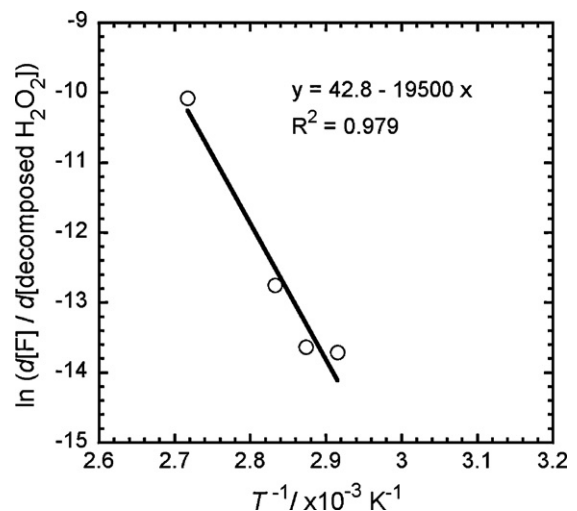
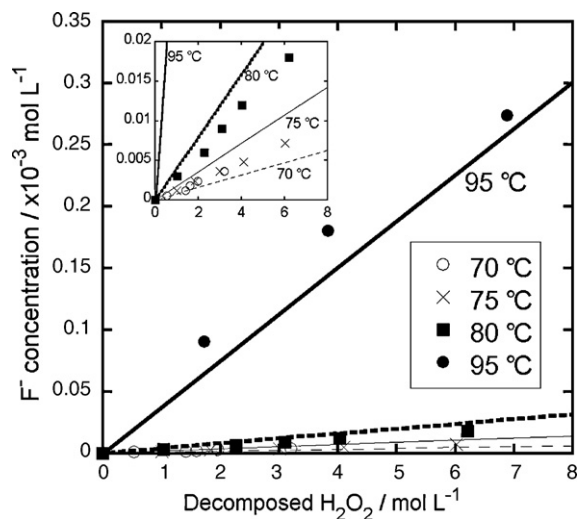


Fig. 9. Natural logarithmic rate of  $\text{H}_2\text{O}_2$  decomposition and fluoride ion concentration as a function of inverse temperature.



**Fig. 10.** Comparison of the real data plots in Fig. 8 with the simulated line from the relationship  $\ln(d[F^-]/d[\text{decomposed H}_2\text{O}_2]) = -19.5 \times 10^3 \text{ K}^{-1} + 42.8$  in Fig. 9. The reaction temperatures are 70 °C (○), 75 °C (×), 80 °C (■), and 95 °C (●).

temperature, as an Arrhenius plot (Fig. 9). There are obvious correlations. These plots can be fitted to a logarithmic approximation with a correlation factor of 0.98. The formula for this approximation is expressed as

$$\ln \left( \frac{d[F^-]}{d[\text{decomposed H}_2\text{O}_2]} \right) = -19.5 \times 10^3 \text{ K}^{-1} + 42.8$$

In Fig. 10, the relations between the fluorine ion concentration and  $\text{H}_2\text{O}_2$  consumption are simulated from the reaction temperature and compared with the actual data. The plots and lines indicate actual data and simulated data from the formula. There is a good correlation between the simulations and the actual data. From this relationship, we can determine the  $\text{H}_2\text{O}_2$  consumption and the fluorine ion concentration at any instant using the fluorine ion concentration and the  $\text{H}_2\text{O}_2$  data, and the reaction temperature.

#### 4. Conclusions

The oxidative degradation of poly fluoroionomers of Nafion was investigated using the relationship between  $\text{H}_2\text{O}_2$  concentration and fluorine ion concentration in the Fenton reaction. The rate of  $\text{H}_2\text{O}_2$  decomposition resulting from reduction by  $\text{Fe}^{2+}$  in aqueous solution was fitted to the pseudo-first-order rate constant, and the reaction rate constant was shown to follow the Arrhenius equation. The activation energy for decomposition of  $\text{H}_2\text{O}_2$  was slightly different in the presence of a Nafion film. The reaction with Nafion had a stronger temperature dependence and a higher reaction rate constant in the temperature range of 60–95 °C. The fluorine ion concentration increased with decreasing  $\text{H}_2\text{O}_2$  concentration. The rate constant for the decrease in fluorine groups from Nafion fitted a pseudo-first-order rate and the reaction also followed the Arrhenius equation. The Nafion surface was morphologically damaged as a result of the Fenton reaction and the surface roughness was reaction temperature dependent.  $\text{H}_2\text{O}_2$  consumption and fluorine ion concentration had an almost linear correlation. The proportional constant obtained from the approximation line had a clear temperature dependence. This relation was expressed by an approximation equation including the temperature, fluorine ion concentration, and  $\text{H}_2\text{O}_2$  concentration. If the fluorine ion concentration and  $\text{H}_2\text{O}_2$  concentration of the exhaust liquid from the PEFC are substituted into the equation, the degradation conditions

of the Nafion film at a given working temperature can be estimated from Arrhenius plots of  $\text{H}_2\text{O}_2$  degradation and fluorine ion production.

#### Acknowledgements

We thank Mr. Sota Takanezawa and Mr. Yusuke Maeda for their valuable discussions. This work was partly supported by Strategic International Cooperative Program, Japan Science and Technology Agency (JST).

#### Appendix A. Supplementary data

Supplementary data associated with this article can be found, in the online version, at doi:10.1016/j.jpowsour.2010.10.043.

#### References

- [1] S. Pylypenko, T.S. Olson, N.J. Carroll, D.N. Petsev, P. Atanassov, *J. Phys. Chem. C* 114 (2010) 4200–4207.
- [2] H. Tawfik, K. El-Khatib, Y. Hung, D. Mahajan, *Ind. Eng. Chem. Res.* 46 (2007) 8898–8905.
- [3] T. Kinumoto, M. Inaba, Y. Nakayama, K. Ogata, R. Umabayashi, A. Tasaka, Y. Iriyama, T. Abe, Z. Ogumi, *J. Power Sources* 158 (2006) 1222–1228.
- [4] W. Schmittinger, A. Vahidi, *J. Power Sources* 180 (2008) 1–14.
- [5] R. Borup, J. Meyers, B. Pivovar, Y.S. Kim, R. Mukundan, N. Garland, D. Myers, M. Wilson, F. Garzon, D. Wood, P. Zelenay, K. More, K. Stroh, T. Zawodzinski, J. Boncella, J.E. McGrath, M. Inaba, K. Miyatake, M. Hori, K. Ota, Z. Ogumi, S. Miyata, A. Nishikata, Z. Siroma, Y. Uchimoto, K. Yasuda, K. Kimijima, N. Iwashita, *Chem. Rev.* 107 (2007) 3904–3951.
- [6] M.S. Sulek, S.A. Mueller, C.H. Paik, *Electrochem. Solid-State Lett.* 11 (2008) B79–B82.
- [7] D.A. Steven, J.R. Dahn, *Carbon* 43 (2005) 179–188.
- [8] S.D. Knights, K.M. Colbow, J. St-Pierre, D.P. Wilkinson, *J. Power Sources* 127 (2004) 127–134.
- [9] K. Hiroshima, T. Asaoka, T. Noritake, Y. Ohya, Y. Morimoto, *Fuel Cells* 2 (2002) 31–34.
- [10] U.A. Paulus, A. Wokaun, G.G. Scherer, T.J. Schmidt, V. Stamenkovic, V. Radmilovic, N.M. Markovic, P.N. Ross, *J. Phys. Chem. B* 106 (2002) 4181–4191.
- [11] A.P. Young, J. Stumper, S. Kinghts, E. Gyenge, *J. Electrochem. Soc.* 157 (2010) B425–B436.
- [12] J. Qiao, M. Saito, K. Hayamizu, T. Okada, *J. Electrochem. Soc.* 153 (2006) A967–A974.
- [13] T. Madden, D. Weiss, N. Cipollini, D. Condit, M. Gummalla, S. Burlatsky, V. Atrazhev, *J. Electrochem. Soc.* 156 (2009) B657–B662.
- [14] V.A. Sethuraman, J.W. Weidner, A.T. Haug, L.V. Protsailo, *J. Electrochem. Soc.* 155 (2008) B119–B124.
- [15] N. Ramaswamy, N. Hakim, S. Mukerjee, *Electrochim. Acta* 53 (2008) 3279–3295.
- [16] T. Aoki, A. Matsunaga, Y. Ogami, A. Maekawa, S. Mitsushima, K. Ota, H. Nishikawa, *J. Power Sources* 195 (2010) 2182–2188.
- [17] A.C. Fernandes, E.A. Ticianelli, *J. Power Sources* 193 (2009) 547–554.
- [18] M. Inaba, T. Kinumoto, M. Kiriake, R. Umabayashi, A. Tasaka, Z. Ogumi, *Electrochim. Acta* 51 (2006) 5746–5753.
- [19] M. Inaba, M. Sugishita, J. Wada, K. Matsuzawa, H. Yamada, A. Tasaka, *J. Power Sources* 178 (2008) 699–705.
- [20] S. Kundu, L.C. Simon, M.W. Fowler, *Polym. Degrad. Stab.* 93 (2008) 214–224.
- [21] K. Matsuoka, S. Sakamoto, K. Nakato, A. Hamada, Y. Itoh, *J. Power Sources* 179 (2008) 560–565.
- [22] H. Tang, S. Peikang, S.P. Jiang, F. Wang, M. Pan, *J. Power Sources* 170 (2007) 85–92.
- [23] C. Chen, T.F. Fuller, *Polym. Degrad. Stab.* 94 (2009) 1436–1447.
- [24] M. Danilczuk, A. Bosnjakovic, M.K. Kadirov, S. Schlick, *J. Power Sources* 172 (2007) 78–82.
- [25] A. Bosnjakovic, S. Schlick, *J. Phys. Chem.* 108 (2004) 4332–4337.
- [26] T. Xie, C.A. Hayden, *Polymer* 48 (2007) 5497–5506.
- [27] A.A. Shah, T.R. Ralph, F.C. Walsh, *J. Electrochem. Soc.* 156 (2009) B465–B484.
- [28] A. Pozio, R.F. Silva, M. De Francesco, L. Giorgi, *Electrochim. Acta* 48 (2003) 1543–1549.
- [29] D. Curtin, R. Lousenberg, T. Henry, P. Tangeman, M. Tisack, *J. Power Sources* 131 (2004) 41–48.
- [30] K. Miyatake, Y. Chikashige, E. Higuchi, M. Watanabe, *J. Am. Chem. Soc.* 129 (2007) 3879–3887.
- [31] L. Merlo, A. Ghielmi, L. Cirillo, M. Gebert, V. Arcella, *J. Power Sources* 171 (2007) 140–147.
- [32] A. Kabasawa, J. Saito, K. Miyatake, H. Uchida, M. Watanabe, *Electrochim. Acta* 54 (2009) 2754–2760.
- [33] C. Chen, G. Levitin, D.W. Hess, T.F. Fuller, *J. Power Sources* 169 (2007) 288–295.
- [34] S. Zhang, X. Yuan, H. Wang, W. Merida, H. Zhu, J. Shen, S. Wu, J. Zhang, *Int. J. Hydrogen Energy* 34 (2009) 388–404.